Transverse-mode selective resonant grating-mirrors for high power and high brightness emission

Nikolay Lyndin, Thomas Kämpfe, Svetlen Tonchev, Stephanie Reynaud, Olivier Parriaux

▶ **To cite this version:**

Nikolay Lyndin, Thomas Kämpfe, Svetlen Tonchev, Stephanie Reynaud, Olivier Parriaux. Transverse-mode selective resonant grating-mirrors for high power and high brightness emission. Optics Express, 2015, 23 (13), pp.17275-17289. 10.1364/OE.23.017275 . hal-01174104

HAL Id: hal-01174104
https://hal.science/hal-01174104

Submitted on 8 Jul 2015

HAL is a multi-disciplinary open access archive for the deposit and dissemination of scientific research documents, whether they are published or not. The documents may come from teaching and research institutions in France or abroad, or from public or private research centers.

L'archive ouverte pluridisciplinaire **HAL**, est destinée au dépôt et à la diffusion de documents scientifiques de niveau recherche, publiés ou non, émanant des établissements d'enseignement et de recherche français ou étrangers, des laboratoires publics ou privés.

Transverse-mode selective resonant grating-mirrors for high power and high brightness emission

Nikolay Lyndin,[1] Thomas Kämpfe,[2] Svetlen Tonchev,[2,3] Stephanie Reynaud[2] and Olivier Parriaux[2,*]

[1]*Prokhorov General Physics Institute of the RAS, Vavilov Street 38, 119991 Moscow, Russia*
[2]*Laboratoire Hubert Curien UMR 5516, 18 rue Professeur Benoît Lauras, Université de Lyon, 42000 Saint-Etienne, France*
[3]*On leave from the ISSP of the Bulgarian Academy of Sciences, 72 Tzarigradsko Chaussee, 1784 Sofia, Bulgaria*
[*]*olivier.parriaux@univ-st-etienne.fr*

Abstract: The finite angular spectral width of a 2D resonant grating mirror is adjusted to select the fundamental transverse mode of a laser and to filter out higher order modes. The selection principle is explained phenomenologically on a simplified 1D model. The 2D design is made so as to sustain the large field concentration in the grating slab-waveguide mirror, and the technology permitting to obtain the resonant reflection within the gain bandwidth of two types of laser is described. The blank experimental measurements by means of a white light supercontinuum are shown to match the targeted specifications on the resonance spectral position and angular width.

©2015 Optical Society of America

OCIS codes: (050.0050) Diffraction and gratings; (130.0130) Integrated optics; (140.0140) Lasers and laser optics.

References and links

1. O. Parriaux, A. V. Tishchenko, and F. Pigeon, "Associating a lossless polarizing function in multilayer laser mirrors by means of a resonant grating," Proc. SPIE **6187**, 72–79 (2006).
2. N. Destouches, J. C. Pommier, O. Parriaux, T. Clausnitzer, N. Lyndin, and S. Tonchev, "Narrow band resonant grating of 100% reflection under normal incidence," Opt. Express **14**(26), 12613–12622 (2006).
3. I. A. Avrutsky, G. A. Golubenko, V. A. Sychugov, and A. V. Tishchenko, "Spectral and laser characteristics of a mirror with a corrugated waveguide on its surface," Sov. J. Quantum Electron. **16**(8), 1063–1065 (1986).
4. G. A. Golubenko, A. S. Svakhin, V. A. Sychugov, and A. V. Tishchenko, "Total reflection of light from a corrugated surface of a dielectric waveguide," Sov. J. Quantum Electron. **15**(7), 886–887 (1985).
5. J. R. Leger, D. Chen, and Z. Wang, "Diffractive optical element for mode shaping of a Nd:YAG laser," Opt. Lett. **19**(2), 108–110 (1994).
6. N. Lyndin, O. Parriaux, A. Tishchenko, and J. F. Bisson, "Mirror structure and laser device comprising such a mirror structure," PCT Patent WO/2007/071794 (2007).
7. E. Popov, L. Mashev, and D. Maystre, "Theoretical study of the anomalies of coated dielectric gratings," Opt. Acta (Lond.) **33**(5), 607–619 (1986).
8. N. M. Lyndin, V. A. Sychugov, A. V. Tishchenko, and B. A. Usievich, "Analytical methods and apparatus employing an optical sensor device with refractive index modulation," US patent No 6218194 B1 (2001).
9. J. F. Bisson, N. Lyndin, K. I. Ueda, and O. Parriaux, "Enhancement of the mode area and modal discrimination of microchip lasers using angularly selective mirrors," IEEE J. Quantum Electron. **44**(7), 628–637 (2008).
10. D. Pietroy, O. Parriaux, and J. L. Stehle, "Ellipsometric retrieval of the phenomenological parameters of a waveguide grating," Opt. Express **17**(20), 18219–18228 (2009).
11. A. Aubourg, M. Rumpel, J. Didierjean, N. Aubry, T. Graf, F. Balembois, P. Georges, and M. A. Ahmed, "1617 nm emission control of an Er:YAG laser by a corrugated single-layer resonant grating mirror," Opt. Lett. **39**(3), 466–469 (2014).
12. I. A. Avrutsky and V. A. Sychugov, "Reflection of a beam of finite size from a corrugated waveguide," J. Mod. Opt. **36**(11), 1527–1539 (1989).
13. N. Lyndin, "MC Grating," *http://www.mcgrating.com*.
14. M. Abdou Ahmed, J. C. Pommier, F. Pigeon, and O. Parriaux, "Flux resistance degradation in resonant grating multilayer mirror," Proc. SPIE **5250**, 229–233 (2004).
15. S. Tonchev and O. Parriaux, "Bypassing and cutting through 1D photonic crystals by ultra-shallow wet-etched resonant gratings," Photonics Nanostruct. Fundam. Appl. **10**(4), 651–656 (2012).

#237706 Received 8 Apr 2015; revised 26 May 2015; accepted 6 Jun 2015; published 24 Jun 2015
© 2015 OSA

16. J. F. Bauters, M. J. R. Heck, D. D. John, J. S. Barton, C. M. Bruinink, A. Leinse, R. G. Heideman, D. J. Blumenthal, and J. E. Bowers, "Planar waveguides with less than 0.1 dB/m propagation loss fabricated with wafer bonding," Opt. Express **19**(24), 24090–24101 (2011).
17. M. M. Vogel, M. Rumpel, B. Weichelt, A. Voss, M. Haefner, C. Pruss, W. Osten, M. A. Ahmed, and T. Graf, "Single-layer resonant-waveguide grating for polarization and wavelength selection in Yb:YAG thin-disk lasers," Opt. Express **20**(4), 4024–4031 (2012).
18. S. Tonchev, T. Kämpfe, and O. Parriaux, "High efficiency, high selectivity ultra-thin resonant diffractive elements," Opt. Express **20**(24), 26714–26724 (2012).

1. Introduction

After having demonstrated the polarization [1] and wavelength (or longitudinal mode) [2] selectivity properties of resonant reflection from a waveguide grating for the control of laser emission, the authors of the present paper are completing here the exploration and exploitation of these waveguide grating properties with the last, and still to be demonstrated, optical function of transverse mode selection. The first scientific demonstration of laser emission control by means of a waveguide grating as a selective laser mirror was made in 1986 by Sychugov et al. [3] short after they identified and analyzed this resonant reflection mechanism as a specific feature of the suitably designed excitation of a grating coupled slab waveguide mode by a free-space wave [4].

The control of the transverse mode spectrum of a laser is an important function which is usually performed by lengthening the laser cavity and restricting the aperture of the laser mirror [5] either by limiting the mirror diameter or by achieving a radial reflectivity gradient matching the dominant transverse mode profile. Such a geometrical approach is not without penalty since it imposes a long laser cavity and does not prevent the dominant transverse mode from suffering losses. Bringing the mirror closer restricts the laser beam diameter, thus the power that the laser can emit in a single transverse mode regime. Resonant reflection from a waveguide grating mirror exhibits this specific and highly useful characteristics that it represents a filter of the transverse modes in the angular spectrum, thus permitting the angularly selective mirror to be placed close to the active medium without limiting the emitting laser area with the most important consequence that the laser power can be extracted from a wide pumped area while achieving higher order transverse mode filtering out. Such mode filtering mirror can thus achieve high power and high brightness all at once with a short cavity length [6].

The specific issues that must be addressed in the implementation of the effect of grating waveguide resonant reflection for the purpose of laser emission control are, first, the limitation of the field concentration in the waveguide to prevent a degradation of the mirror's damage threshold, secondly, a waveguide grating uniformity over a range larger than the propagation distance of the mode in the grating waveguide, thirdly, the achievement in the grating mirror's angular spectrum of a spectral width larger than that of the fundamental transverse mode and smaller than that of the next higher order transverse mode, and finally a spectral position of the waveguide grating resonance under normal incidence within the gain bandwidth of the considered laser system.

The present paper reports on the design (Section 2), the waveguide grating technology and the blank characterization measurements of two different mirror structures (Section 3): one for an erbium-doped microchip laser emitting in the C-band, and one for a high power Yb:YAG disk laser at 1030 nm wavelength ("blank characterization" of the mirrors stands here for the measurement outside the laser resonator of their selectivity properties). These mirror structures represent two examples where the optical function of transverse mode selection can be beneficially implemented.

2. Design of the transverse-mode selective mirrors

2.1 Operation principle in a 1-D waveguide grating

Grating-mediated resonant reflection of a plane wave impinging on a lossless slab waveguide reaches 100% theoretically [7]. As this reflection effect relies upon the excitation of a waveguide mode, it is angularly selective and can therefore in principle be used to provide

#237706 Received 8 Apr 2015; revised 26 May 2015; accepted 6 Jun 2015; published 24 Jun 2015
© 2015 OSA

close to 100% reflection for a beam of definite angular spectral width while a beam of wider angular width would experience a smaller reflection. This property was already used by the authors in the design of an evanescent wave biosensor where the resonance angle monitors the bioreaction taking place at the surface of the grating waveguide [8]. Considering now the said beam as that amplified in a laser cavity, and therefore normal incidence, its characteristics depend on the type of amplifying medium and on the related conformation of the laser resonator. One usually distinguishes two types of laser resonators: stable and unstable resonators. There are correspondingly two distinct transverse mode filtering schemes performing the same function of reflecting a beam of defined angular width while partially transmitting beams of wider angular spectrum. In the first scheme, corresponding to a stable laser resonator whose mirror operation is symbolically represented in Fig. 1 in a 1D geometry, the angular reflection width of the resonant mirror is designed to be larger than the angular width of the dominant transverse mode of the laser cavity and smaller than that of the higher order transverse mode. Consequently, the fundamental mode experiences close to 100% reflection whereas the higher order modes experience a reflection which sets them below the lasing threshold. This mirror is used as the rear mirror of the laser resonator, the standard front mirror ensuring the coupling of the laser energy outside the cavity in the form of the transverse mode selected by the rear mirror. There is here the implicit hypothesis that this laser system has low thermal lensing which is the case for instance in disk lasers where the cooling is made homogeneously over the whole disk surface.

In laser systems where the thermal lensing is strong as in microchip lasers for instance, the transverse mode filtering function is implemented in the front mirror and operates as follows [9]: the resonant mirror is designed to highly reflect an incident wave having large extent and narrow angular width (close to a plane wave) which the high gain active medium amplifies and also distorts. Upon the few subsequent reflection events on the resonant mirror the plane wave component of the amplified beam is again reflected while the distorted amplified components are transmitted through the coupler and represent the diffraction limited laser output since their angular spectrum is outside the angular width of the resonant mirror. The output wave does not correspond to the fundamental transverse mode here: it is a higher order transverse mode whose spatial coherence is high and can be converted to a diffraction limited beam by external free-space wave elements.

The rationale of resonant grating filtering in a stable resonator configuration is first explained in a simplified 1D grating model as illustrated in Fig. 1 where the wave coupling phenomenology is well developed: it is known since 1985 [3] that resonant reflection of theoretically 100% of an incident free-space wave from a grating slab waveguide is the result of the destructive interference in the transmission medium of the transmitted 0th order superposed to the wave coupled by the grating to a waveguide mode then reradiated by the grating into the adjacent media. Two conditions must be fulfilled for this destructive interference to occur: first, the waveguide mode synchronism condition (usually via the −1st order of the grating of period Λ) must be satisfied at wavelength λ which writes:

$$k_0(\sin q + n_e) = K_g \tag{1}$$

where $k_0 = 2\pi/\lambda$, $K_g = 2\pi/\Lambda$, θ is the incidence angle and n_e is the effective index of the waveguide mode at wavelength λ. The second condition concerns the grating strength described by the radiation coefficient α which determines the propagation length $L = 1/\alpha$ of the mode in the grating waveguide: for the spatial overlap of the two waves interfering destructively in the transmission medium to be substantial, the propagation length L must be smaller than the projection of the incident beam diameter in the waveguide plane. The angular width of resonant reflection $\Delta\theta$, i.e., the angular range at constant wavelength over which the reflection coefficient is larger than 50% is inversely proportional to L and estimated as $\Delta\theta = \alpha\lambda$ The phenomenological analysis of resonant reflection under oblique incidence with the relationships between phenomenological parameters and optogeometrical parameters is exhaustively given in [10].

#237706 Received 8 Apr 2015; revised 26 May 2015; accepted 6 Jun 2015; published 24 Jun 2015
© 2015 OSA

The configuration which prevails in a laser resonator is most often normal incidence on the mirror as illustrated in Fig. 1. Resonant reflection also occurs under normal incidence [2]. The waveguide coupling synchronism condition now writes from (1) $\Lambda = \lambda/n_e$, but the propagation length L, which determines the angular width, now depends on the radiation coefficient α and, per symmetry, also and notably on the second order intra-guide coupling coefficient κ between the forward and backward propagating mode which tends to reflect it back, thus to decrease the propagation length in the waveguide and consequently to widen the angular width of resonant reflection regardless of its spectral width. This property of resonant reflection under normal incidence permits to adjust the angular and wavelength spectral widths essentially independently unlike in the well known usual case of oblique incidence as used by Aubourg et al. to improve the beam quality of an Er:YAG laser [11] and first demonstrated in a laser by Avrutsky [12]. This combined effect of α and κ implies that no simple analytical expression can be given for L, thus for $\Delta\theta$, in the normal incidence case, the more so as the phenomenological parameters α and κ loose their usefulness as they vary substantially with the optogeometrical parameters in the neighborhood of normal incidence. This however is not a big difficulty since $\Delta\theta$ can be calculated numerically, for instance by using exact modal or Chandezon codes [13] and the propagation length by $L = \lambda/\Delta\theta$.

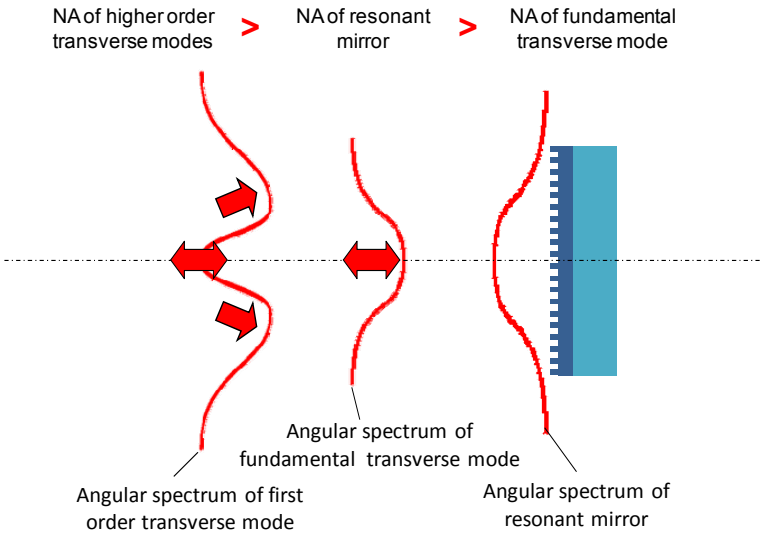

Fig. 1. Sketch of a laser grating-mirror with 1D representation of the angular width $\Delta\Phi_0$ of the fundamental and higher order transverse mode $\Delta\Phi_1$ relative to that of the resonant mirror for the filtering out of the high order transverse modes.

Having found the angular width $\Delta\theta$ of resonant reflection, it is time now to fit it between the angular width $\Delta\Phi_0$ and $\Delta\Phi_1$ of the dominant and first higher order transverse modes so as to ensure high, close to 100% reflection for the fundamental mode and a reflection below the lasing threshold for the first higher order transverse mode. $\Delta\Phi_0$ and $\Delta\Phi_1$ as well as the beam diameter are determined by the laser cavity. Figure 1 illustrates schematically the relationship between the angular widths involved.

2.2 Two-D waveguide grating mirrors: specific problems and conditions

The transposition from the above simplified 1D model to the actual model of a 2D grating is not straightforward. The same rationale applies, but the structure design cannot be made as an inverse problem assisted with a meaningful phenomenological representation. It is made on the basis of the four conditions hereafter and frequent resort to an exact 2D grating code [13].

A *first design condition* results from the requirement of a translation- and rotation-invariant mirror element. The requirement of azimuthally symmetrical resonant reflection

#237706 Received 8 Apr 2015; revised 26 May 2015; accepted 6 Jun 2015; published 24 Jun 2015
© 2015 OSA

states that the dependence of the reflection coefficient R($\Delta\theta$) on the incidence angle around normal incidence is identical whatever the azimuth of the incidence plane in the grating waveguide plane. For the angular filtering to be azimuthally and translation independent, the most adequate 2D grating pattern is that of a hexagonal set of holes (or pillars). This is however not a sufficient condition for obtaining an azimuthally symmetrical angular spectrum of the resonant reflection: the symmetry of the waveguide corrugation plays an important role as illustrated vividly in Figs. 3(a)–3(d) corresponding to the transverse mode selective mirror for a *disk laser* described in Section 4. For instance, if the corrugation is symmetrical, i.e., if the corrugation (e.g., the set of holes) is first made in the substrate by etching, then the waveguide slab is deposited onto the latter, defining at its upper side a nearly conformal corrugation, we could not obtain a circularly symmetrical angular spectrum as shown in Figs. 3(a) and 3(b) which illustrate in a grey scale the dependence of the reflection coefficient versus the two incidence angles α_G and α_I under TE and TM incidence respectively (TE and TM incidence is defined as usual relative to the incidence plane and corresponds to the "s" and "p" polarizations) and coupling to the only propagating TE_0 waveguide mode. Figure 2 illustrates the incident geometry of the 2D angular reflection graphs with the angles α_G and α_I as defined in the used modeling codes [13].

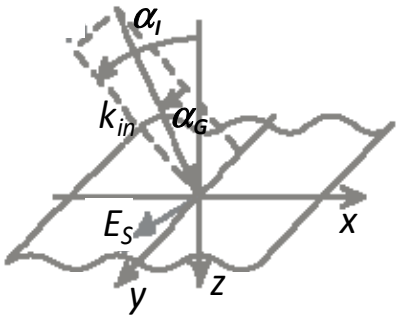

Fig. 2. Incidence geometry with definition of the scanning angles around normal incidence used in subsequent figures.

The azimuthal dependence of the angular width of the resonant reflection is far from constant which implies that a waveguide grating with two conformally corrugated boundaries does not exhibit angularly invariant reflection. Now, if the corrugation is only defined at the upper side of the waveguide, the substrate side being flat, it is possible to find the conditions for an almost circular angular spectrum as shown in Figs. 3(c) and 3(d) for TE and TM incidence respectively by coupling to the sole TE_0 waveguide mode.

Under the approximation of small angles around the normal, $\alpha_I = \sin^{-1}(k_x/k_{in})$ and $\alpha_G = \sin^{-1}(k_y/k_{in})$ where k_{in} is the modulus of the wave vector of the incident wave in air and k_x and k_y its projections along axes x and y. It is worth noting that an azimuthally symmetrical angular spectrum like that of Fig. 3(c) with TE incidence favors the resonant reflection of a laser beam of azimuthal polarization distribution while that of Fig. 3(d) favors that of a radially polarized incident beam. Thus, the same mirror, with the excitation of the same TE_0 waveguide mode, exhibits a different transverse-mode selectivity for radially and azimuthally polarized beams. Which polarization distribution will be emitted by a laser having such transverse-mode filtering front mirror cannot be anticipated; this will depend on the laser resonator, the beam diameter and related transverse-mode spectrum, and can only be analyzed experimentally.

#237706 Received 8 Apr 2015; revised 26 May 2015; accepted 6 Jun 2015; published 24 Jun 2015
© 2015 OSA

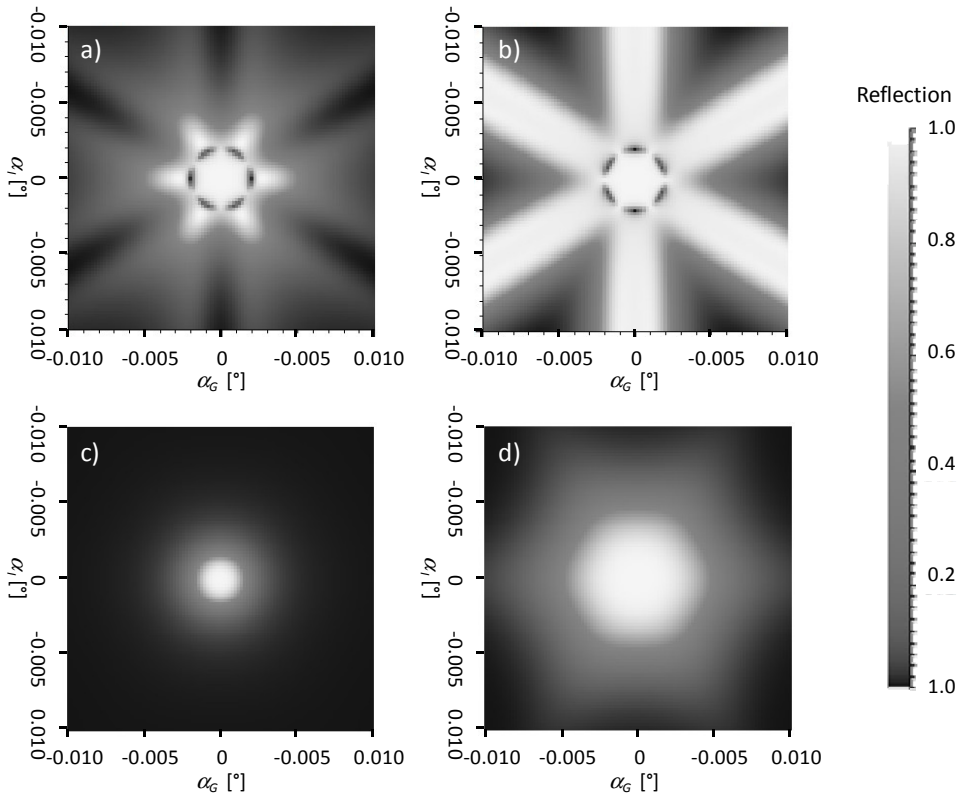

Fig. 3. 2D angular spectra of the reflection from a slab waveguide with hexagonal set of holes designed for a disc laser mirror sketched in Fig. 9 upon excitation of the only propagating TE_0 mode: a) TE incident polarized and b) TM polarized excitation by a double-sided corrugation, c) TE and d) TM excitation by a single-sided corrugation.

The *second design condition* in the present work is thus: the corrugation must be single-sided. This configuration represents a difficulty for the technology to achieve high uniformity: having a conformal double-sided corrugation would guarantee an inherently excellent uniformity of the waveguide mode effective index n_e since the waveguide thickness would everywhere be the same, whereas with a single corrugation, any non-uniformity in the hole depth and diameter will affect the effective index uniformity, thus the phase of the propagating waveguide mode, therefore the build up of the modal field in the waveguide and the very possibility to achieve close to the theoretical 100% resonant reflection.

The need for a single-sided corrugation will also be illustrated in the case of the *microchip laser* application whose structure and operation is described in Section 3 and related figure. The specifications on the beam diameter (i.e. on the modal propagation length), and the power resistance are here much less demanding, therefore the waveguide mode used for resonant reflection does not have to be as close to cutoff as the mode in the *disk laser* mirror whose cross-section is shown in the cross-section figure of Section 4.

#237706 Received 8 Apr 2015; revised 26 May 2015; accepted 6 Jun 2015; published 24 Jun 2015
© 2015 OSA

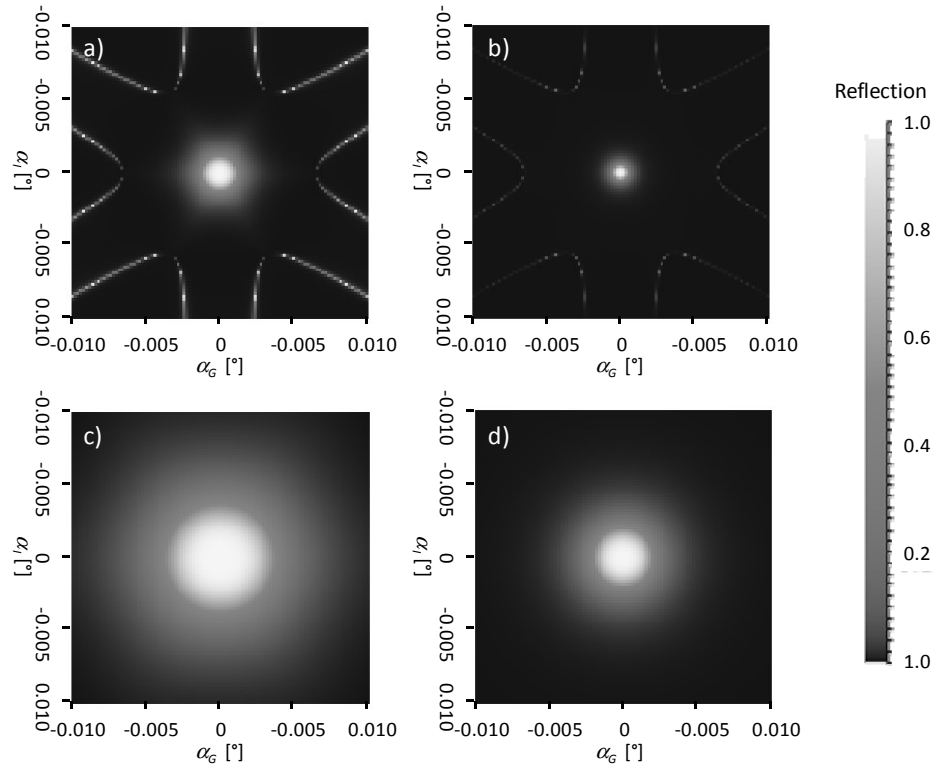

Fig. 4. 2D angular spectrum of the reflection from an hexagonal set of holes of the back-mirror sketched in Fig. 5 designed for a microchip laser with TM_0 mode excitation. Curves a) and b): TE and TM incident polarization onto a multilayer system where all interfaces have conformal undulation. Curves c) and d): TE and TM incident polarization with single-sided undulation of the upper waveguide boundary.

The waveguide in Fig. 5 propagates the TE_0 and also the TM_0 mode. The grating strength in the *microchip laser* is notably larger than in the *disk laser* case (Section 4) since the corrugation is made directly in the high index waveguide slab; nevertheless the angular spectra corresponding to the TE_0 mode excitation are qualitatively similar to those of Fig. 3 and will therefore not be illustrated. For sake of completeness however, we are showing in Fig. 4 the angular spectra resulting from the excitation of the TM_0 mode of the waveguide although the fabricated structure described in Section 3 will be designed for the TE_0 mode excitation. Figures 4(a) and 4(b) show that with TM_0 mode coupling the useful width of the angular spectrum is extremely narrow (about 0.01 degree), and that a single-sided corrugation, as in Figs. 4(c) and 4(d) the angular width is still too small (0.04 and 0.02 degree for TE and TM incidence respectively) for a microchip laser beam of less than 1 mm cross-section. This generally small angular width with TM_0 mode coupling is an effect of the radiation coefficient of a TM mode normally to the grating waveguide surface being small as its normal modal electric field component - which is large - radiates zero field normally to the grating waveguide surface. That is why coupling to the TE_0 mode is preferred here too, with the angular width of 0.1 and 0.2 degree for the TE and TM incident polarizations respectively.

A *third design condition* is made in the objective of keeping a high damage threshold despite the high field accumulation in the waveguide mode. Whereas a single waveguide layer with grating can alone ensure in principle 100% reflection as shown in the very first demonstration of the effect in a laser mirror application [3], the field accumulation will lead to a notable fall of the damage threshold [14] (this will be discussed further quantitatively in Section 4). The solution to this is to make a division of function between a non-selective first submirror in the form of a wide-band standard multilayer ensuring most of the reflection, and

#237706 Received 8 Apr 2015; revised 26 May 2015; accepted 6 Jun 2015; published 24 Jun 2015
© 2015 OSA

a highly selective resonant submirror completing the reflection, integrated to the latter but placed at the exit side of the laser mirror. Still in the objective of further limiting the field accumulation in the waveguide mode, the mode is set close to its cutoff, the waveguide being quasi-symmetrical, i.e., the low index buffer layer between the multilayer and resonant sub-mirrors and the thick waveguide cover layer having the same refractive index. This will be used in the transverse mode selective Yb:YAG *disk laser* front mirror since such lasers are often used for high power laser machining.

A *fourth design condition* is to design the grating waveguide resonant submirror with quasi-zero reflection off-resonance in order to obtain a quasi-symmetrical reflection peak. To that end, the waveguide may be composed of number of high and low index layers ensuring antireflection properties outside the resonance.

3. Transverse-mode selective microchip-laser back mirror

3.1 Resonant mirror structure and fabrication

The aim is here to enable the single transverse-mode lasing in the C-band (1530-1565 nm wavelength) of an ytterbium and erbium co-doped microchip-laser of relatively large area of the order of one millimeter in order to achieve both high power and high brightness by means of a resonant grating mirror integrated to the microchip. The resonant mirror is placed at the side of the 980 nm wavelength pump at which it exhibits close to 100% transmission, i.e. close to zero diffraction loss despite the propagating character of the 1st diffraction orders at the pump wavelength. As sketched in Fig. 5, the multilayer submirror is composed of alternate low (SiO_2) and high (Ta_2O_5) index layers ensuring about 90% non-selective reflection at 1535 nm wavelength, and the waveguide layer of 94.7 nm thickness is made of Ta_2O_5, the set of holes being etched into the latter with a cover layer to make the modal field close to symmetrical. Although the present microchip laser application is less critical than the disk laser application regarding laser damage, a special care is taken to limit the power density in the Ta_2O_5 waveguide by making it symmetrical and close to cutoff. The corrugation at the uppermost interface in Fig. 5 has no optical function; it is the result of the conformal ion plating deposition of the last SiO_2 layer after the waveguide grating has been etched. As shown at the end of this Section, exact modeling leads to a 0.5 degree angular spectral width with the following parameters: the period of the hexagonal set of holes is 1112 nm (minimum spacing between holes equal to the hole diameter) with 34.4 nm depth in the Ta_2O_5 waveguide layer.

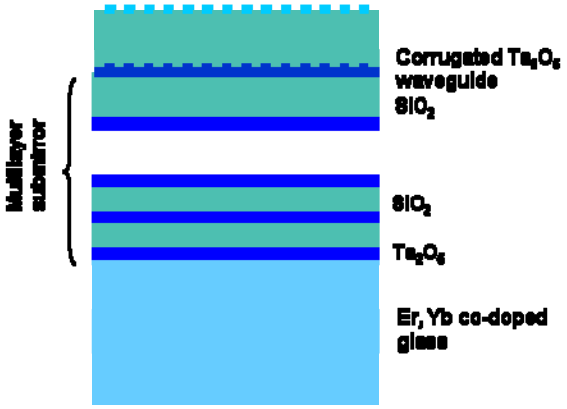

Fig. 5. Corrugated layer stack of the rear resonant mirror of a microchip laser.

The definition of the hole pattern is first made by e-beam in a chromium mask which is then transferred into a photoresist layer by hard contact. The technology chosen for the physical transfer of the holes into the Ta_2O_5 waveguide layer is slow wet etching which had to be specifically developed [15]. This technological step is extremely critical since the single-

#237706 Received 8 Apr 2015; revised 26 May 2015; accepted 6 Jun 2015; published 24 Jun 2015
© 2015 OSA

side corrugation is made in the waveguide layer where the modal field is maximum, any error and non-uniformity on the hole depths and diameters translating into a non-uniform deviation of the effective index from its assigned value. Dry etching was excluded because no standard reactive dry process exists for Ta_2O_5 permitting the reproducible etching of so shallow a corrugation with a precision of + - 3 nm as required for the resonance to be close enough to the targeted wavelength of 1535 nm. It was anticipated that the use of reactive ion beam etching with its combined action of chemical and physical effects would not permit the requested accuracy. Figure 6 is the 2D AFM scan of a few holes having the requested depth of 34.4 nm + - 3 nm.

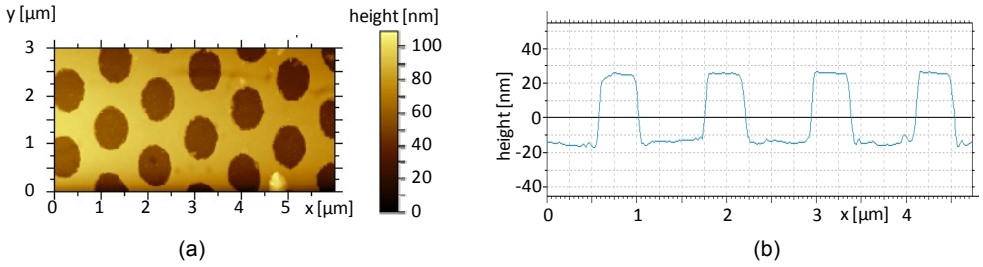

Fig. 6. 2D AFM scan (a) and 1D line scan (b) of the set of holes of Fig. 5 after wet etching into the Ta_2O_5 waveguide layer.

3.2 Blank characterization

The blank characterization of the optical function of the structure was first made before depositing the last symmetrization layer of SiO_2 in order to keep the possibility of resonance trimming by adjusting the thickness of the latter. A fiber white light supercontinuum in a transmission measurement scheme permits to achieve a 0.5 nm resolution on the wavelength of the resonant reflection and 1 mrad on the angular width. Remarkably, all 34 fabricated samples exhibit a resonance wavelength within a 8 nm range around the central wavelength of 1479.5 nm before the cover deposition with an angular width within about 30 mrad full width. Figure 7 gives the wavelength spectrum of the transmission under normal incidence of a typical mirror element without cover layer showing a FWHM of 3 nm. Exact modeling was resumed to evaluate the thickness of the SiO_2 cover permitting to reach the desired operation wavelength of the microchip laser after deposition. After the deposition of this last cover layer on top of the set of holes, the final measurement reveals that the 31 samples submitted to the deposition process have their resonance within a 1526 – 1538 nm range; it was checked experimentally that, for a given sample, the wavelength spectrum is little dependent on the incident linear polarization orientation. Figure 8(a)) shows the theoretical angular spectra obtained under TE and TM incidence (TE and TM are defined relative to the plane in which the angular scan is made) with coupling to the TE_0 guide mode for both cases. A typical experimental angular scan of the transmission obtained with a linearly polarized incident beam is shown in Fig. 8(b): the angular FWHM is 1.6 degrees, i.e., about 8 times the theoretically expected angular width of 0.2 degrees. This broadening of the angular width is attributed to the too wide angular window used in the experimental angular scanning and to some scattering loss of the waveguide grating; it is not due to a non-uniformity of the set of holes since the transmission dip in Fig. 8 is close to zero which means that the resonant reflection mechanism operates properly.

#237706 Received 8 Apr 2015; revised 26 May 2015; accepted 6 Jun 2015; published 24 Jun 2015
© 2015 OSA

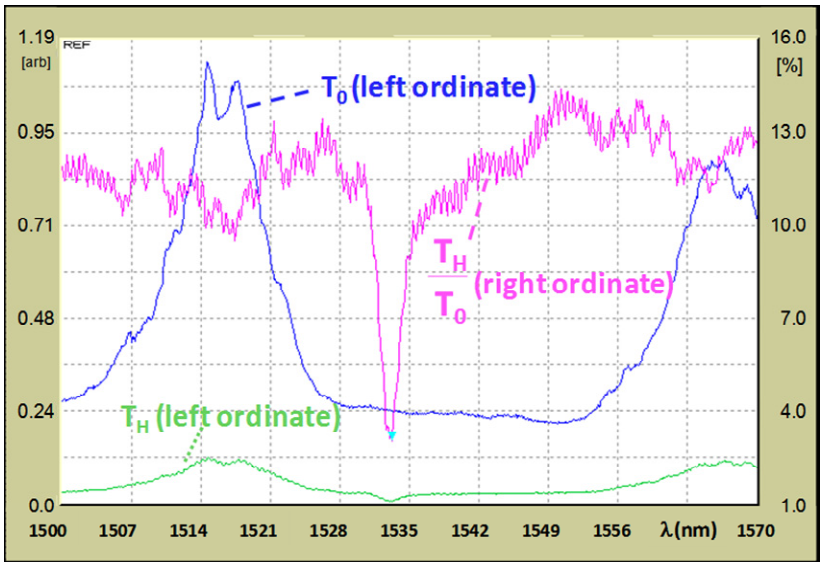

Fig. 7. Wavelength scan in the C-band of the transmission under normal incidence and linear polarization of one of the 31 mirrors fitting the specifications (T_0: transmission in region without the hexagonal grating, T_H: transmission with hexagonal grating)

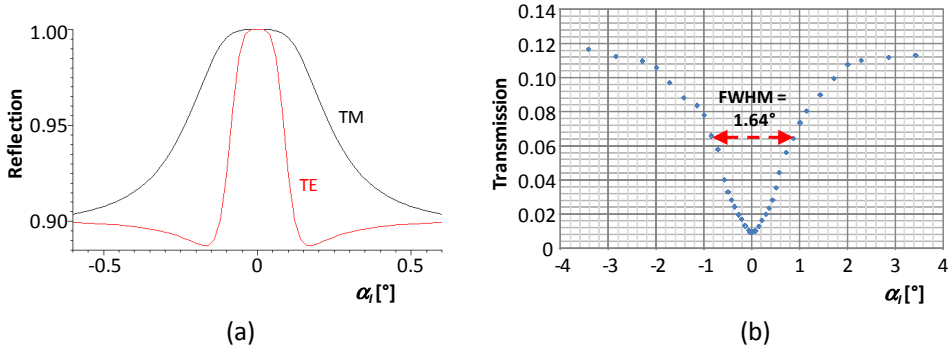

Fig. 8. Angular scans of one of the resonant mirrors with cover layer at its maximum reflection at 1535 nm wavelength under quasi-normal TE incidence. (a) Reflection modeling for both TE (red curve) and TM (black curve) incidence with TE_0 mode coupling. (b) Measured angular spectrum of the transmission under TE incidence.

4. Transverse mode selective Yb:YAG high power disk laser front mirror

4.1 Resonant mirror structure and fabrication

The aim is here to decrease the M^2 number of a high power Yb:YAG disk laser at 1030 nm wavelength for a beam of a few millimeter diameter. The resonant mirror is here the output coupler. The standard multilayer submirror ensuring 95% non-selective reflection is deposited at the outer side of a thick fused quartz substrate in the form of 7 quarter wave layers of Ta_2O_5 and SiO_2. The resonant submirror is at the outer side of a standard 0.5 mm thickness fused quartz substrate. It consists of a 52.6 nm thick LPCVD Si_3N_4 waveguide layer annealed by the very low-loss technology of Lionix [16] covered by a LPCVD SiO_2 cover layer of 253 nm thickness. As sketched in Fig. 9, the non-selective multilayer submirror and the resonant waveguide submirror are later assembled by wafer direct bonding (WDB). This post-assembling is required since high quality and high uniformity LPCVD silicon nitride can only

#237706 Received 8 Apr 2015; revised 26 May 2015; accepted 6 Jun 2015; published 24 Jun 2015
© 2015 OSA

be deposited on fused quartz wafers of standard thickness and does not result from design considerations

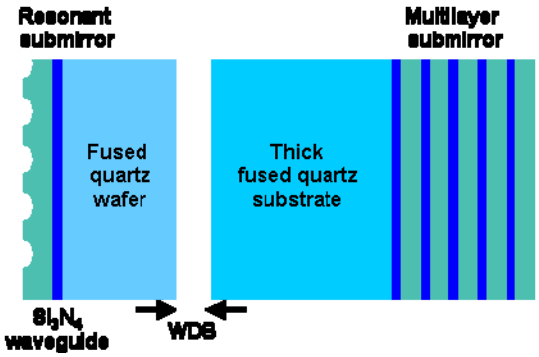

Fig. 9. Bonded assembly of non-selective and resonant submirrors as a disk laser output mirror.

The quasi-symmetric Si_3N_4 waveguide has a TE_0 mode effective index of 1.458 assuming a substrate and cover index of 1.45, i.e., it is close to its cutoff which means that the field accumulation in the waveguided mode is moderate, and that it is likely to sustain high power laser emission. The modal electrical field maximum in the waveguide was estimated theoretically by modeling the whole structure including resonant and multilayer submirrors as shown in Fig. 9. The power reflection coefficient of the isolated multilayer submirror is 95%. Figure 10 represents the electric field modulus distribution of the coupled TE_0 mode in the silicon nitride waveguide at resonance under normal incidence over one period of the 2D grating. The black circles indicate the position of the holes. For an incident wave with electric field parallel to the x-axis the same field component E_x in the silicon nitride waveguide has its maximum under the holes as shown in Fig. 10(a) while if the electric field of the incident wave is parallel to the y-axis, the corresponding field component E_y has an additional maximum between holes as shown in Fig. 10(b). The field distribution at resonance is actually very complex and what can be learned from Fig. 10 is where the weak points of the structure regarding the power flux resistance are and it is clear that the hot spots are in the waveguide under the holes. Not shown in Fig. 10 is the dependence of the field magnitude across the waveguide slab; the field maximum is reached at about 15 nm from the bottom waveguide boundary. The maximum maximorum of the electric field modulus in the waveguide is about 10 times the incident field modulus (see the grey scale of Fig. 10 defining the electric field modulus relative to the incident field modulus), i.e., 10 times the field modulus in the laser cavity. This maximum electric field was chosen so that the operation point of the element is below the known damage threshold of about 1 J/cm^2 of current high index layer materials.

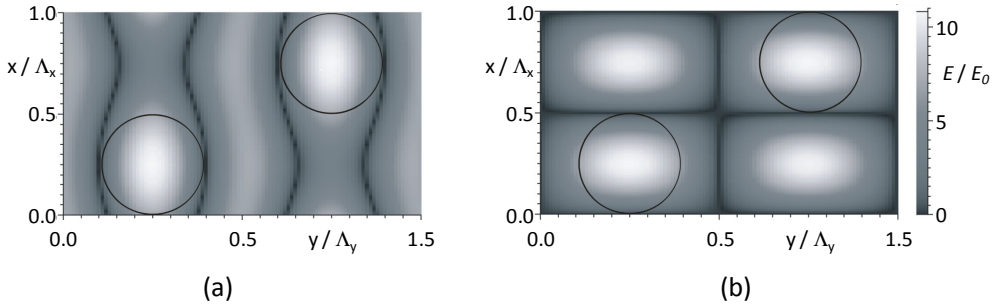

Fig. 10. TE_0 modal electric field modulus distribution over one period in the Si_3N_4 waveguide of the element of Fig. 9 at resonance under normal incidence of a x-polarized wave. The black circles indicate the position of the holes at the upper surface of the cover layer. (a) Modulus of the x component of the electric field, (b) of its y component.

#237706 Received 8 Apr 2015; revised 26 May 2015; accepted 6 Jun 2015; published 24 Jun 2015
© 2015 OSA

An interesting comparison can be made before such mirror is tested in a laser cavity: in principle, a laser mirror composed of the sole waveguide grating, without the multilayer submirror, would give rise to the desired transverse-mode selectivity as originally shown more than 25 years ago [3] and tested recently as the polarizing mirror of a moderate power laser [17]. The electric field modulus maximum in the case of the sole resonant waveguide grating with the same transverse-mode selection property would be much larger and lead to a maximum power density in the waveguide 40 times larger than in the present multilayer-assisted element. The question may be raised as to the possible detrimental role of the thick (several millimeters) low index buffer between the two highly reflective submirrors as a rather high Q Fabry-Perot resonator. In its operation as a laser mirror, the assembled element ensures that the field reflected by the multilayer submirror and the field reflected by the resonant submirror interfere constructively toward the active medium of the laser. It turns out that under this condition there is no energy accumulation in the Fabry-Perot which also means that the condition for energy accumulation in the Fabry-Perot corresponds to a reflection below the lasing threshold.

Exact modeling leading to the angular spectra of Figs. 3(c) and 3(d) delivers the following parameters: the period of the hexagonal set of hole is 816 nm (minimum spacing between holes equal to hole diameter) with 57.3 nm depth in the SiO_2 cover layer.

The definition of the hole pattern is first made by e-beam in a chromium mask which is also transferred into a photoresist layer by hard contact. The technology chosen for the physical transfer of the holes into the SiO_2 cover layer is a slow wet etching process as well which had to be specifically developed [18]. The reasons for choosing wet etching are the same as in Section 3: the need for precise nanometer control of the etch depth of so shallow holes. Figure 11 is the SEM image of the photoresist corrugation and Fig. 12 is the AFM 2D-scan of a few holes having the requested depth of 57.3 nm + - 3 nm.

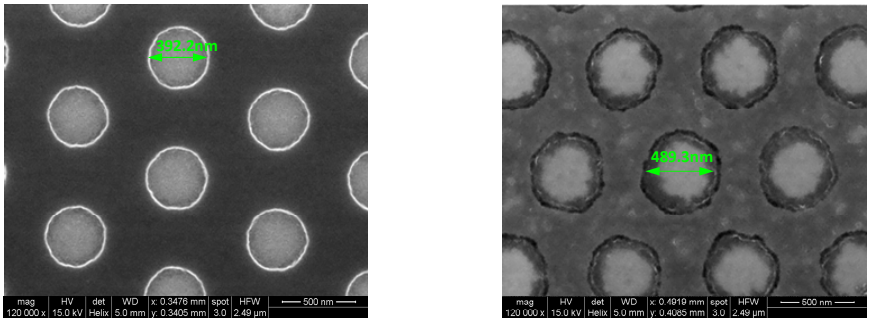

Fig. 11. (a) SEM image of a set of developed holes of 816 nm period in a ~120 nm thick photoresist layer, (b) same set of holes after wet etching into the SiO_2 layer.

#237706 Received 8 Apr 2015; revised 26 May 2015; accepted 6 Jun 2015; published 24 Jun 2015
© 2015 OSA

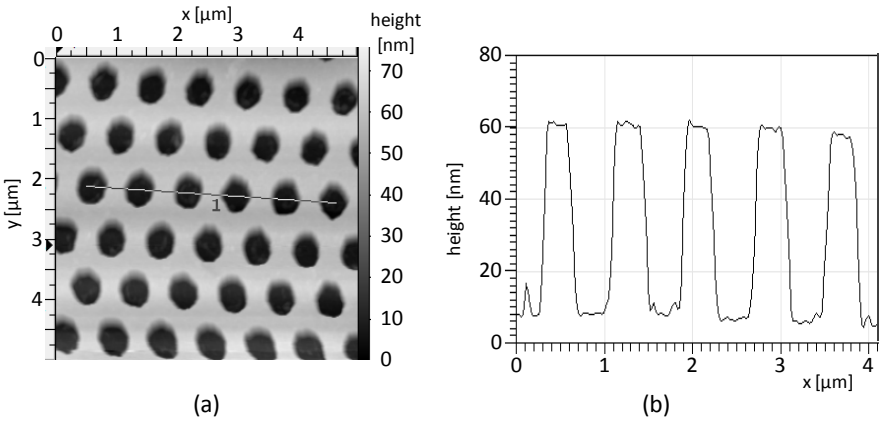

Fig. 12. (a) 2D AFM scan of the set of holes of Fig. 11 after wet etching into the SiO_2 cover layer, (b) 1D profile scan of a) showing the grating height.

4.2 Blank characterization

The blank characterization of the optical function of the resonant submirror was made in transmission with the same white light super continuum source. Remarkably again, all fabricated 15 samples exhibit a resonance wavelength within a 3 nm range around a central wavelength of 1028.5 nm. The resonance in this case is so narrow that the depth of the dip in the spectral transmission as well as in the angular response is significantly reduced in the experimental setup, due to the limited spectrometer resolution of 0.5 nm and the incidence angle variation due to residual divergence of about 0.06° of the white light beam used for illuminating the grating. The effects of those variations of the parameters of the optical setup on the reflection spectra are shown in Fig. 13. Varying the incidence angle from normal incidence to 0.05° gives rise to a pair of peaks for each considered angle in the wavelength spectrum which are separated by about 1 nm. Besides, varying the wavelength by ± 0.1 nm off the designed resonance wavelength of 1030 nm gives rise in the angular spectrum to a double peak separated by about 0.1° for shorter wavelengths, while at longer wavelengths the resonance shape remains but exhibits a reduction of the maximal transmission down to about 15%.

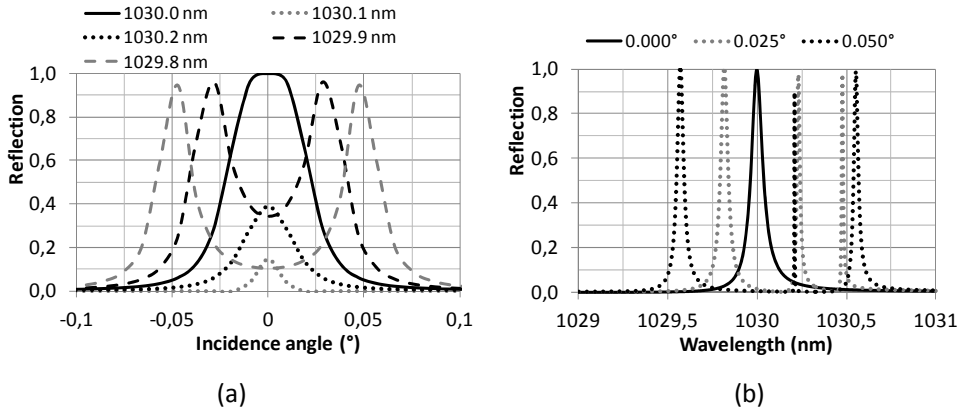

Fig. 13. Simulation of the transmission wavelength and angular spectrum of the mirror. (a) Wavelength spectrum for 3 incidence angles close to normal incidence. (b) Angular spectrum for five wavelengths close to the design-wavelength of 1030 nm.

#237706 Received 8 Apr 2015; revised 26 May 2015; accepted 6 Jun 2015; published 24 Jun 2015
© 2015 OSA

A simulation was made taking both spectral width effects into account by calculating the response of the grating for a 2D scan of wavelength and incidence angle, followed by a 2D integration of the calculated reflection values with a Gaussian weight distribution representing the 0.5 nm spectrometer resolution and the 0.06° beam divergence. The resulting transmission curves are shown in Fig. 15. They agree well with the experimental results.

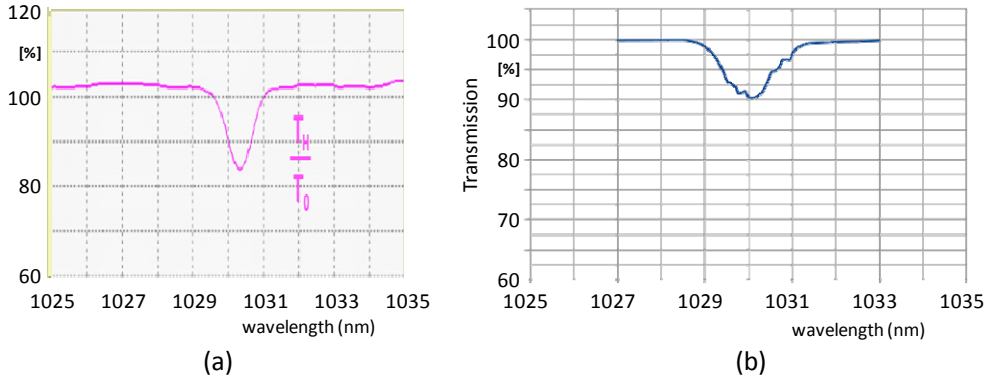

Fig. 14. Wavelength scan of the transmission of a resonant submirror for linearly polarized incidence. (a) Measured transmission graph for a spectrometer resolution of 0.5 nm and a beam divergence of 0.06°, corrected for substrate backside reflection (b) Simulation of the transmission taking into account the spectrometer resolution and beam divergence of the experiment.

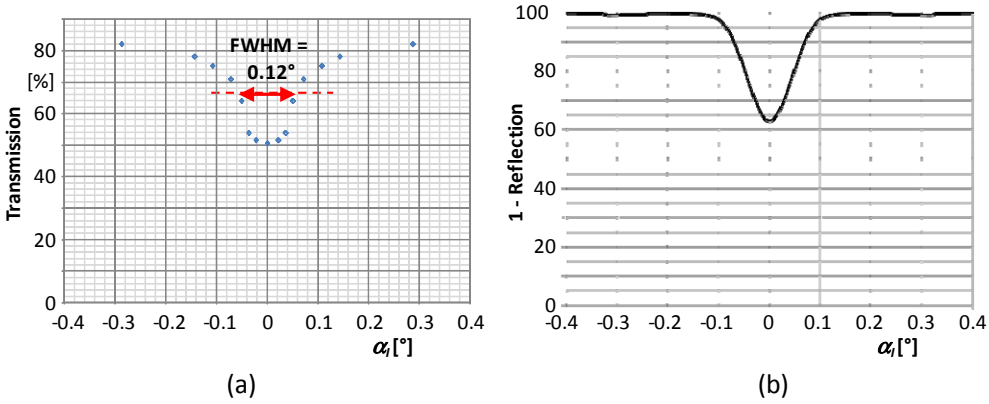

Fig. 15. Angular scan of the transmission of a resonant submirror for linearly polarized incidence. (a) Measured transmission for a spectrometer resolution of 0.5 nm and a beam divergence of 0.06°, not corrected for backside reflection. (b) Simulation of the transmission taking into account the spectrometer resolution and beam divergence from the experiment, without backside reflection.

The fact that the transmission is close to 100% off-resonance in Figs. 14 and 15 results from the fact that the experimental measurement of transmission is made on the resonant submirror of Fig. 9 before WDB with the multilayer submirror.

Although the Lionix LPCVD Si_3N_4 waveguide technology on fused quartz gives rise to extremely low scattering losses below 1 dB per meter [16], the fabrication constraints of the present element (its unusually large thickness, the demand on parallelism) did not permit to use standard microelectronic fused quartz wafers and to fully exploit the low-loss potential of this technology. The latter is however within reach and can be used at a later stage once the optical function has been demonstrated in a disk laser.

#237706 Received 8 Apr 2015; revised 26 May 2015; accepted 6 Jun 2015; published 24 Jun 2015
© 2015 OSA

5. Conclusion

The present paper has developed the design and the fabrication technology for the demonstration of the last selectivity property of resonant reflection from a waveguide grating which has not been demonstrated yet: transverse mode filtering. Exact 2D modeling based on the phenomenological understanding of 1D structures has led to discarding the waveguide grating configurations not permitting a circularly symmetrical angular filtering and to the optimization of those which achieve azimuthal independence. Two different mirrors have been designed for the two most interesting wavelength ranges of 1030 nm and the C-band, each being optimized for the beam size and highest laser flux resistance. Specific technology processes have been developed to match the extremely critical specifications on the resonance spectral position and on the angular width of the resonance; these solutions can be further stabilized to become manufacturing technologies for the present functional elements as well as more generally for all resonant diffractive elements. The blank experimental results confirm a posteriori the design and technological choices made and enable now the functionality tests as mirrors of laser cavities.

Acknowledgment

The present work was made with the support of LST Lyon Science Transfert under project number L770.

#237706 Received 8 Apr 2015; revised 26 May 2015; accepted 6 Jun 2015; published 24 Jun 2015
© 2015 OSA